Author(s): Poli, F. M.; Podestà, M.; Fasoli, A.

Article Title: A robust method for measurement of fluctuation parallel wavenumber in laboratory plasmas
Year of publication: 2009
Link to published version:
http://dx.doi.org/10.1063/1.3125627
Publisher statement: None

A robust method for measurement of fluctuation parallel wavenumber in laboratory plasmas

F.M. Poli,* M. Podestà,† and A. Fasoli

CRPP-EPFL, Association EURATOM-Confédération Suisse, Lausanne, Switzerland

(Dated: October 21, 2009)

Abstract

Measuring the parallel wavenumber is fundamental for the experimental characterization of electrostatic instabilities. It becomes particularly important in toroidal geometry, where spatial inhomogeneities and curvature can excite both drift instabilities, whose wavenumber parallel to the magnetic field is finite, and interchange instabilities, which typically have vanishing parallel wavenumber. We demonstrate that multipoint measurements can provide a robust method for the discrimination between the two cases.

*Electronic address: f.m.poli@warwick.ac.uk; Present address: Department of Physics, University of Warwick, Gibbet Hill road, Coventry, CV4 7AL, UK

†present adress: Department of Physics and Astronomy, University of California, Irvine 92697, CA USA

I. INTRODUCTION

Devices for basic plasma physics experiments in linear and toroidal geometry are used worldwide to study the properties of electrostatic instabilities [1]-[8] and their transition to turbulence [9]-[10]. For some regimes drift and flute (or *interchange*) modes co-exist [11]-[13], and a correct identification of the nature of the instability is therefore essential. A number of properties are commonly used to infer the nature of an instability from experimental data. These include the dispersion relation, both perpendicular and parallel to the magnetic field, the associated phase velocity across the magnetic field, the phase shift between density and plasma potential fluctuations [14]. However, for non-vanishing temperature fluctuations or highly nonlinear fluctuations, the phase shift is not univocally defined and may lead to ambiguous results [13]. The dispersion relation across the magnetic field is often similar for pure drift and drift-interchange instabilities, and it cannot be used to discriminate between the two. Moreover, Doppler corrections due to the fluid $\mathbf{E} \times \mathbf{B}$ velocity can be much larger than the phase velocity itself, and the estimate of the latter is strongly affected by experimental uncertainty. In contrast, $k_\parallel$ is unique for drift and interchange instabilities [15]. Its accurate measurement is therefore critical for a correct identification of the instabilities. In principle, $k_\parallel$ can be extracted from the phase difference between fluctuations - for example in the density - measured by a pair of probes separated along the magnetic field. Examples of measurement of wavenumber, correlation length, cross-coherence and cross-phase along the magnetic field in tokamaks and basic plasma physics devices are given in Refs. [16]-[17]. In those experiments one probe was fixed and the other was scanned along z. In practice, the probes can never be perfectly aligned, so that the measurement can be affected by the projection of $k_\perp \gg k_\parallel$ along the direction of measurement, leading to an overestimate of $k_\parallel$. In addition, probes with finite size act as a high-pass filter in k-space [18], making the measurement untrustful for small values of $k_\parallel$. It is therefore difficult to discriminate between a small but finite $k_\parallel$ associated with drift (including drift-interchange) waves in plasmas with small ion Larmor radius and a vanishing $k_\parallel$ associated with flute instabilities. Probe arrays are less sensitive to these negative effects, and have been used, for example, to reconstruct the three dimensional nature of drift wave turbulence [19]. In addition, they can provide information on the full dispersion relation (along the magnetic field and perpendicular to it) in a single discharge and at different locations. For example, a reconstruction of the

radial vs perpendicular dynamics is important to investigate the transfer of energy due to nonlinear, quadratic interactions, since the 'frozen flow hypothesis' may fail if the condition $k_R \ll k_z$ is violated, as discussed in [10]. As a drawback, probes may represent a stronger perturbation to the plasma. Perturbations can be minimized in basic plasma devices such as TORPEX (see Sec. II), in which, typically, the ion Larmor radius is substantially larger than the probe size [20][21]. This is achieved by optimizing the distance between the tips of a probe array and the toroidal displacement between probes. Therefore, although a two-point measurement is less perturbative, the reconstruction of the parallel wavenumber using a fix probe and an array of probes is more precise and robust, providing coherent measurements of fluctuations over an extended region for a single plasma discharge. In this paper it is shown that, by using arrays of Langmuir probes the effect of $k_\perp$ on the measurement can be isolated and the value of $k_\parallel$ can be extracted unambiguously.

II. EXPERIMENTAL SETUP AND METHOD

The experiments presented herein are performed in the toroidal device TORPEX [7] (major radius $R_0 = 1$ m, minor radius 0.2 m), in Hydrogen plasmas at a neutral gas pressure of 6×10^{-5} mbar. The helical magnetic field lines result from the superposition of a dominant toroidal component $B_\phi < 100$ mT, and a small vertical component $B_z \leq 4$ mT. Plasmas are generated and sustained by microwaves injected from the low field side, with a frequency of 2.45 GHz, in the range of the electron cyclotron frequencies [22][23]. Typical time-averaged parameters are density $\sim 10^{16} - 10^{17}$ m^{-3}, electron temperature ~ 5 eV and plasma potential $\sim 10 - 20$ V.

A cylindrical reference frame is used in the following, where R is the major radius, z is the vertical coordinate with respect to the midplane and ϕ is the toroidal angle. Figure 1 shows the arrangement of the probes used to measure the dispersion relation on TORPEX. One array (S) has eight tips with mutual separation of 1.8 cm, with tip #1 being located at midplane. This movable array is commonly used in sweeping mode for the measurement of the time-averaged plasma parameters over the region $|R - R_0| \leq 12$ cm and $|z| \leq 13$ cm. The second array (T) has twelve tips arranged in a 4×3 grid, with horizontal separation of 1 cm and vertical separation of 1.8 cm, with tips #1-4 being located at midplane. This array can be used in sweeping mode for the measurement of the radial pressure gradients

and of the radial electric field. The arrays S and T are located respectively at positions O' and O on the equatorial plane and separated by $\overline{OO'} = R\Delta\phi$, with $\Delta\phi = \pi/2$. The following considerations enter in the choice of the toroidal distance between arrays. First, it has to be long enough that the probes can be considered point-like with respect to their mutual distance, as also discussed in [18]. Second, it has to be short enough that the level of coherence in the range of frequencies of interest is sufficiently high, but yet the probes are not 'shielding' each other. On TORPEX, measurements performed with a third array, positioned at $2\pi/3$ from array S, revealed in some cases, especially in plasma configurations where the degree of turbulence is high, a reduction of the coherence by a factor of three. The toroidal separation between arrays is therefore optimized in order to minimize the errors introduced in the measurements by the finite probe size, yet maintaining high the coherence even in the presence of high degree of turbulence.

The directions of $k_\parallel$ and $k_\perp$ are shown in Fig. 1(c), with $k_\parallel$ along the magnetic field and $k_\perp$ on the plane perpendicular to it. Taking O as the reference position, there is a magnetic field line passing through O that intersects the array S, whose z coordinate, measured with respect to the equatorial plane, is:

$$z_0 = R\Delta\phi\frac{B_z}{B_\phi}, \tag{1}$$

Both arrays can rotate around their shaft, on a plane perpendicular to R. In the following derivation it is assumed that the array T is kept vertical, while the array S can assume an arbitrary angle α with respect to the positive z axis, as shown in Fig. 1(b). The direction of the measured wavenumber, indicated in Fig. 1(c) as k_m, will be a combination of $k_\parallel$ and $k_\perp$. Due to the low ratio of $k_\parallel$ to $k_\perp$, the measurement can be strongly affected by the projection of $k_\perp$ along the direction of measurement.

Indicating with γ the angle between the direction of measurement and the z axis, the measured wavenumber is:

$$k_m = k_\parallel \cos\gamma \pm k_\perp \sin\gamma \tag{2}$$

where the positive and negative sign hold respectively for $\alpha > \pi/2$ and for $\alpha < \pi/2$, and $\cos\gamma = (\mathbf{k}_m \cdot \hat{z})/|\mathbf{k}_m|$. Using trigonometric relations, the measured wavenumber k_m can be

written as:

$$k_m(z) = \frac{k_\perp}{\sqrt{1+\left(\frac{z}{L}\right)^2}\sqrt{1+\left(\frac{B_z}{B_\phi}\right)^2}} \times \left[\frac{k_\parallel}{k_\perp} + \frac{B_z}{B_\phi} - \frac{z}{L}\left(1 - \frac{B_z}{B_\phi}\frac{k_\parallel}{k_\perp}\right)\right] \tag{3}$$

where $L = R\Delta\phi + z\tan\alpha$ is the toroidal distance between tips, measured at the midplane. On TORPEX typically $B_z/B_\phi \leq 3\times10^{-2}$ and $k_\parallel/k_\perp < 10^{-2}$. The term $(B_z/B_\phi)(k_\parallel/k_\perp)$ can therefore be neglected with respect to unity. These values for the magnetic field and for the ratio $k_\parallel/k_\perp$ are typical for several basic plasma physics experiments in toroidal geometry (see, for example, Ref. [2] and references therein). Moreover $\sqrt{1+(z/L)^2} \cong 1$, as the correction to unity is $\approx 0.2\%$ at the maximum vertical distance between tips, $\Delta z \sim 11.8$ cm. With these approximations the measured wavenumber finally results to be:

$$k_m \cong k_\parallel + k_\perp\left(\frac{z_0}{L - z\tan\alpha} - \frac{z}{L}\right) \tag{4}$$

For $\alpha = 0, \pi$ (array S vertical) this reduces to:

$$k_m \cong k_\parallel + k_\perp\frac{z_0 - z}{L} \tag{5}$$

Note that $k_m = k_\parallel$ when $z = z_0$. In the case of $k_\parallel = 0$, the measured wavenumber changes its sign crossing the magnetic field line, since the only contribution comes in this case from the projection of $k_\perp$ along the direction of measurement. In general, for $k_\parallel/k_z \ll 1$ and for measurements not taken along the magnetic field line, the measured wavenumber is dominated by the contribution of $k_\perp$. For $k_\parallel \neq 0$ the relative error on the measurement of $k_\parallel$ can be quantified as:

$$\frac{k_m - k_\parallel}{k_\parallel} \cong \frac{k_\perp}{k_\parallel}\frac{z - z_0}{L} \tag{6}$$

The relative error increases with the distance z from the magnetic field line at z_0 because of the projection of $k_\perp$. The linear dependence expressed by Eq. (5) can be used to interpolate the value of the wavenumber at position z_0, which also represents the most accurate estimate of $k_\parallel$. Alternatively, Eq. (5) can be used to infer the value of both $k_\parallel$ and $k_\perp$ from a linear fit of the experimental data. The value of $k_\perp$ obtained from the fit can then be compared to independent measurements of k_z performed in the same plasma and at the same position, for example using two tips of the array T aligned along z. The comparison between the

value of $k_\perp$ from Eq. (5) and independent estimates of k_z from two-point measurements [24] typically shows a good agreement [8].

Measurements with the array S oriented downward, with $|\alpha| < \pi/4$ with respect to the mid-plane, have revealed a strong shadowing effect between tips. Rather than trying to adjust the angle of rotation of the probes to increase the experimental points in the region of z_0, a more accurate estimate of $k_\parallel$ can be obtained by keeping the array S vertical and using Eq. (5) to extract $k_\parallel$.

For each combination of probe pairs from the arrays S and T, we have measured the wavenumber and frequency power spectrum $P(k_m, \omega)$ along the toroidal direction and at various positions along the major radius R, following the method described in Ref. [24]:

$$P(k_m, \omega) = \frac{1}{M} \sum_{j=1}^{M} I_\Delta[k_m^j(\omega) - K] \frac{1}{2} \left[P_S(z_S, \omega) + P_T(z_T, \omega) \right]. \tag{7}$$

Here the sum runs over M independent samples and $P_S(z_S, \omega)$ and $P_T(z_T, \omega)$ are the power spectra computed from the density fluctuations measured respectively using probes S and T at vertical positions z_S and z_T. The wavenumber $k_m^j(\omega)$ is computed from the cross-spectrum between S and T:

$$k_m^j(\omega) = \frac{1}{\sqrt{L^2 + \Delta z^2}} \arg[n_S^{j*}(z_S, \omega) n_T^j(z_T, \omega)] \tag{8}$$

The indicator function I_Δ, the discrete equivalent of the delta function, is defined as:

$$I_{2\Delta}[k_m^j(\omega) - K] = \begin{cases} 1 & K - \Delta \leq k_m^j(\omega) < K + \Delta \\ 0 & elsewhere \end{cases} \tag{9}$$

Computing (7) is equivalent to constructing a histogram: for each sample j, the measured wavenumber $k_m^j(\omega)$ is compared with the reference values of K. The resulting power spectrum provides an indication of the degree of turbulence in the plasma and can be used to estimate the average dispersion relation along the direction of alignment of probes [24].

III. RESULTS

An application of the method described in the previous section is shown here in the case of a drift-interchange instability with $k_\parallel \neq 0$ (Fig. 2), and in the case of an interchange instability, with $k_\parallel = 0$ (Fig. 3). The identification of the nature of electrostatic instabilities on TORPEX has been extensively discussed elsewhere and it is not repeated here [8][13][**?**].

Both drift and interchange modes are observed on TORPEX, with amplitude that depend on the value of the magnetic field connection length, which can be controlled by varying the magnitude of the vertical field component [13]. The toroidal magnetic field is the same in the two cases, $B_\phi = 76$ mT, while the vertical field is $B_z = 0.6$ mT in the first case and $B_z = 1.6$ mT in the second. In both cases a coherent mode is detected in the power spectrum of density fluctuations. This mode is measured both on the high and low field sides in the case of the drift-interchange instability, but only on the low field side in the case of the interchange instability, as shown in the inset in Figs. 2-3. We have measured the wavenumber and frequency spectrum $P(k_m, \omega)$ along the toroidal direction as described in the previous section and fitted the spectrum with a gaussian function to find the central frequency and wavenumber and the spectral width of the mode.

The figures report the values of the coherence spectrum γ^2 measured at the frequency of the mode, computed from cross-measurements between tip #2 of array T and all the eight tips in array S. For both instabilities the value of γ^2 is maximum at a coordinate z closest to the ideal position of the magnetic field line, z_0, indicated in the figures with a dashed line. In the case of the drift mode, as shown in Fig. 2(a), a second maximum is measured in the coherence spectrum at $R - R_0 = -14$ cm, at a vertical distance of approximately 4.5 cm from the first maximum. This position corresponds to the intersection of a field line that passes through the position occupied by the array T after a complete toroidal turn:

$$z_1 = \frac{B_z}{B_\phi} R(\Delta\phi + 2\pi)$$

For the sake of completeness and to increase the statistical significance of the linear fit, also the values of k_m obtained from the cross-phase between array S and tips #6 and #10 in array T have been plotted in the figures. The measured wavenumber is plotted as a function of the vertical distance $\Delta z = z_T - z_S$.

For both instabilities the measured wavenumbers increase linearly with the vertical separation between tips, the slope being a function of $k_\perp$, as from Eq. (5). In the case of the drift-interchange mode, $k_\parallel = 0.21$ m^{-1} at $R - R_0 = -14$ cm and at the vertical position where the coherence is maximum. For comparison, the wavenumber measured at the second maximum of coherence, correcting for the total length of the field line, is 0.16 m^{-1}, comparable with the measurement taken at the absolute maximum of coherence. On the low field side, the interpolation of the value of k_m at z_0 gives $k_\parallel = 0.19$ m^{-1}, in good agreement with

the measurement taken on the high field side.

In the case of the interchange mode, Fig. 3(c), the measured wavenumber changes its sign across z_0, indicating that $k_\parallel$ is close to zero. The value of the wavenumber at the coordinate of maximum coherence spectrum is $k_m \simeq -0.1$ m^{-1}, with a spectral width of 0.1 m^{-1}. An interpolation of k_m at the coordinate z_0, using the parameters of a linear fit of the experimental data, gives $k_\parallel \simeq 0.06$ m^{-1}. Nevertheless, this value is still an overestimate of $k_\parallel$, since systematic errors in the value of the magnetic field and in the exact position of the arrays (both R and α), affect the estimate of z_0, of the distance between tips and therefore the final value of k_m. The error on the distance between tips contribute for less than 6% on the measurement of the parallel wavenumber, while that on the estimate of z_0 has been estimated to be $\Delta z_0 = 0.04 z_0$. Referring to Eq. (1) and (5), the minimum value of $k_\parallel$ that can be inferred from a linear interpolation depends therefore on the value of $k_\perp$ and on the ratio B_z/B_ϕ, namely $k_{min} \sim 0.04 k_\perp B_z/B_\phi$. For typical values of the magnetic field and $k_\perp$, it is obtained a minimum value of approximately 0.03 m^{-1}. We note that the width of the wavenumber spectrum, as estimated from $P(k_m, \omega)$ is anyhow larger than any systematic error and it should be taken as an indication of the possible deviation of $k_\parallel$ from zero. In the example discussed above, with $k_\parallel \simeq 0.06$ m^{-1} at z_0, the width of the wavenumber spectrum at the position of maximum coherence is 0.1 m$^{-1} \gg k_\parallel$. It should be concluded that, within the errors of measurement, and taking into account the degree of turbulence, the parallel wavenumber is vanishing.

To conclude, measurements of the parallel wavenumber based on two probes are affected by large errors due to the contribution of the projection of the perpendicular wavenumber along the direction of measurement. For low values of the ratio of the vertical to toroidal fields, typical of basic plasma physics devices, the dependence of the measured wavenumber on $k_\perp$ is linear. Combining simultaneous cross-phase measurements taken at different vertical positions with probe arrays, the linear dependence on $k_\perp$ can be used to obtain a robust measurement of the value of the parallel wavenumber. Although the advantages of this method are immediate in basic plasma devices, where probes can be moved along the radial direction, multipoint measurements can also be applied to sets of fixed Langmuir probes at the edge of fusion devices. Assessing the dominant character of turbulence, for example whether drift or interchange, is in fact a topic issue for validation of turbulence codes in fusion plasmas and for establishing reliable quantitative predictions for burning plasmas.

Acknowledgments

This work is supported in part by the Swiss National Science Foundation.

---

[1] A. Latten, T. Klinger, A. Piel, and T. Pierre. *Rev. Sci. Instrum.*, **66**, 3254 (1995).

[2] O. Grulke, F. Greiner, T. Klinger, and A. Piel. *Plasma Phys. Control. Fusion*, **43** 525 (2001).

[3] F. J. Oynes, O. M. Olsen, H. L. Pecsely, A. Fredriksen, and K. Rypdal. *Phys. Rev. E*, **57** 2242 (1998).

[4] S. Niedner, B. D. Scott, and U. Stroth. *Plasma Phys. Control. Fusion*, **44** 397 (2002).

[5] C. Schröder, O. Grulke, T. Klinger, and V. Naulin. *Phys. Plasmas*, **12** 42103 (2005).

[6] J. C. Perez, W. Horton, K. Gentle W. L. Rowan, K. Lee, and R. B. Dahlburg. *Phys. Plasmas*, **13** 32101 (2006).

[7] A. Fasoli, B. Labit, M. Mc Grath, S. H. Müller, G. Plyushchev, M. Podestà, and F. M. Poli. *Phys. of Plasmas*, **13** 055902 (2006).

[8] F. M. Poli, S. Brunner, A. Diallo, A. Fasoli, I. Furno, B. Labit, S. H. Müller, G. Plyushchev, and M. Podestà. *Phys. of Plasmas*, **13** 102104 (2006).

[9] M. J. Burin, G. R. Tynan, G. Y. Antar, N. A. Crocker, and C. Holland. *Phys. Plasmas*, **12** 52320 (2005).

[10] F. M. Poli, M. Podestà, and A. Fasoli. *Phys. Plasmas*, **14** 052311 (2007).

[11] F. Brochard, E. Gravier, and G. Bonhomme. *Phys. Plasmas*, 12:62104, 2005.

[12] K Kamataki, S-I Itoh, Y Nagashima, S Inagaki, S Shinohara, M Yagi *et al* *Plasma Phys. Control. Fusion*, **48**, 119, (2003).

[13] F. M. Poli, P. Ricci, A. Fasoli and M. Podestà. *Phys. Plasmas*, **15** 032104 (2008).

[14] D. L. Jassby. *Phys. Fluids*, **15** 1590 (1972).

[15] A. B. Mikhailovskii. *Basic plasma physics*, volume I, pages 587–610. A. Galeev and R. N. Sudan, North Holland, Amsterdam, 1983.

[16] D. L. Winslow, R. D. Benstson, B. Richards, and W. A. Craven. *Rev. Sci. Instrum.*, **68** 397 (1997).

[17] K. Rypdal, and S. Ratynskaia, *Phys. Rev. Letters*, **94** 225002 (2005).

[18] N. Iwama Y. Ohba and T. Tsukishima. *J. Appl. Phys.*, **50** 3197 (1979).

[19] N. Mahdizadeh, F. Greiner, T. Happel, A. Kendl, M. Ramisch, B. D. Scott and U. Stroth, *Plasma Phys. Control. Fusion*, **49** 1005 (2007).

[20] I. H. Hutchinson, *Principles of plasma diagnostics*, Cambridge University Press, New York (1987)

[21] F. F. Chen, in *Plasma Diagnostics techniques*, R. H. Huddlestone and S. L. Leonard editros, Academic Press, New York (1965).

[22] M. Podestà, A. Fasoli, B. Labit, M. Mc Grath, S. H. Müller and F. M. Poli, *Plasma Phys. Control. Fusion*, **47** 1989 (2005).

[23] A. Fasoli, B. Labit, M. Mc Grath, S. H. Müller, G. Plyushchev, M. Podestà, and F. M. Poli, *Plasma Phys. Control. Fusion*, **48** 1053 (2006).

[24] J. M. Beall, Y. C. Kim, and E. J. Powers. *J. Appl. Phys.*, **53** 3933 (1982).

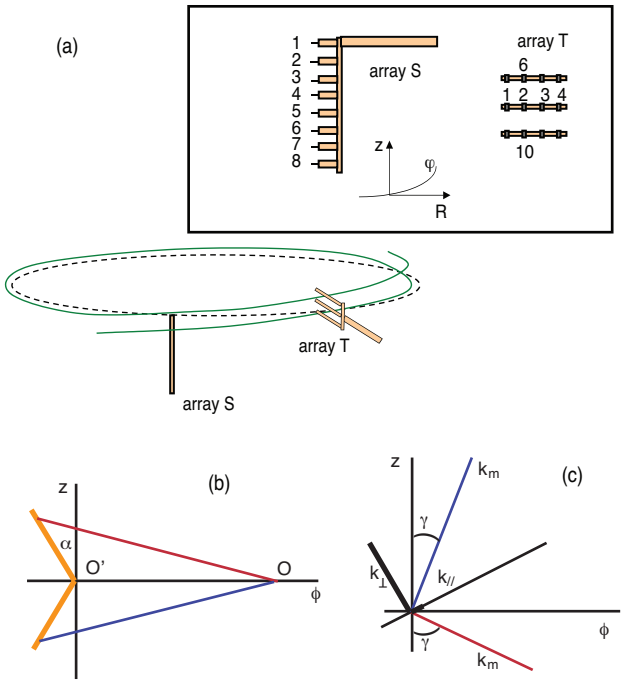

FIG. 1: (a) Geometrical setup for the measurements of the parallel wavenumber. The arrays S and T are positioned at the midplane (black dashed line) and are separated by $\pi/2$ along the toroidal direction. Numbers indicate the tips effectively used for the measurements. The green line indicates the field line that intersects the tip#2 of array T on the midplane, at the toroidal position O. (b) Geometry of probes during the measurement of $k_{\|}$. ϕ and z denote the toroidal and the vertical direction in our cylindrical reference, α is the angle formed by the array S (orange) with the positive z axis. The red and blue line indicate the direction of measurement when the array S is oriented respectively upward and downward. (c) Direction of the measured wavenumber, k_m, when S is oriented downward (blue line) or upward (red line) with respect to the direction of $k_{\|}$ and $k_{\perp}$.

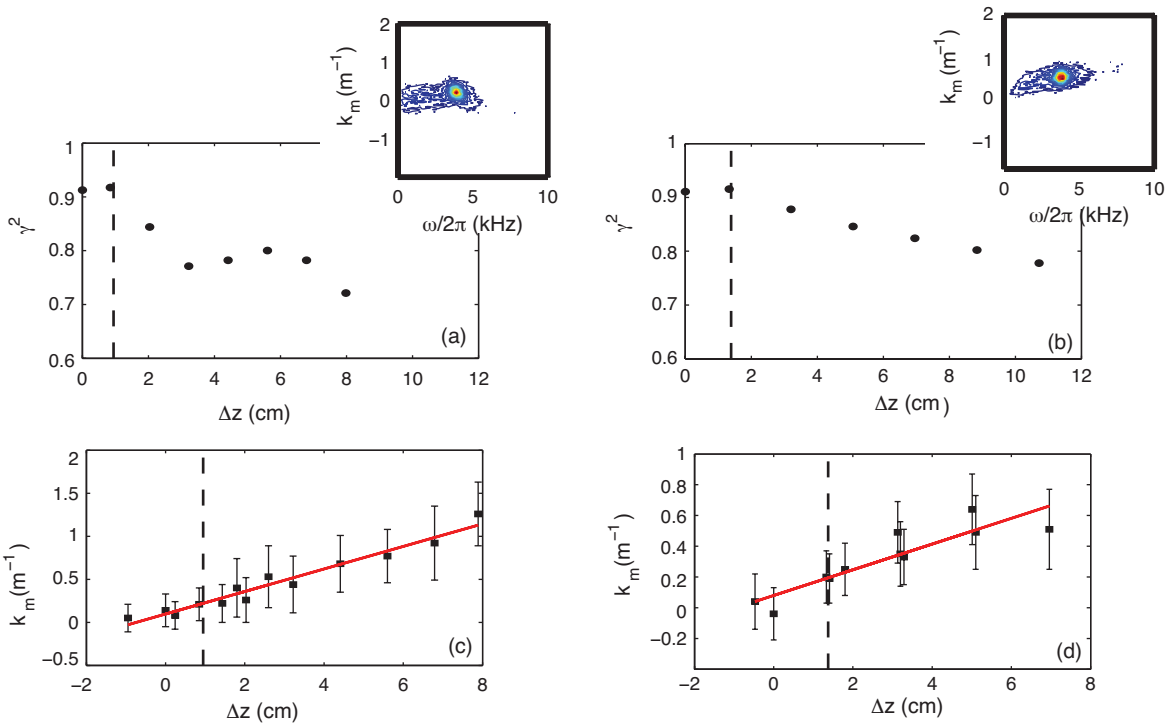

FIG. 2: Top: Value of the coherence spectrum associated with the unstable mode at 4 kHz (see inset), measured between the 8 tips in the array S and tip #2 in array T. Measurements are done at $R - R_0 = -14$ cm (a) and $R - R_0 = 4$ cm (b). Bottom: wavenumber measured with respect to tips #2, 6, 10 of array T, at $R - R_0 = -14$ cm (c) and $R - R_0 = 4$ cm (d). The insets show the power spectrum $P(k_m, \omega)$ measured at the coordinate of the maximum coherence spectrum.

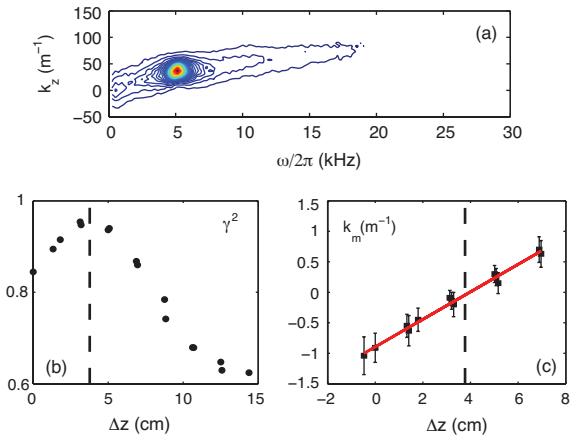

FIG. 3: (a) Power spectrum of density fluctuations measured across the magnetic field $P(k_z, \omega)$ at $R - R_0 = 5$ cm, for $B_z = 1.6$ mT. (b) Variation of the coherence spectrum, calculated at the frequency of the mode, with the vertical separation between tips $\Delta z = (z_T - z_S)$. The dashed line indicates the vertical coordinate z_0 where the magnetic field line passing through the reference tip at the toroidal location O intersects the array S at toroidal position O'. (c) Variation of the measured wavenumber k_m with respect to the vertical separation between tips. The plotted value of k_m is the center of the gaussian curve that fits the wavenumber spectrum $P(k_m)$, the error bar is its spectral width.